


**รายงานวิจัยฉบับสมบูรณ์**

**โครงการ**

# การเตรียมและพัฒนาตัวเร่งปฏิกิริยากลุ่มแพลทินัมขนาดนาโนเพื่อใช้ในปฏิกิริยาแนพทา รีฟอร์มมิง

**โดย**

**ผศ. ดร. โอกร เมฆาสุวรรณดำรงและคณะ**

**มิถุนายน 2553**

สัญญาเลขที่ MRG5180140

รายงานวิจัยฉบับสมบูรณ์

โครงการ

# การเตรียมและพัฒนาตัวเร่งปฏิกิริยากลุ่มแพลทินัมขนาดนาโนเพื่อใช้ในปฏิกิริยาแนพทา รีฟอร์มมิง


ผศ. ดร. โอกร เมฆาสุวรรณดำรง
ภาควิชา วิศวกรรมเคมี
คณะวิศวกรรมศาสตร์และเทคโนโลยีอุตสาหกรรม
มหาวิทยาลัยศิลปากร

ศ.ดร. ปิยะสาร ประเสริฐธรรม
ภาควิชา วิศวกรรมเคมี
คณะวิศวกรรมศาสตร์
จุฬาลงกรณ์มหาวิทยาลัย



สนับสนุนโดยสำนักงานคณะกรรมการการอุดมศึกษา และสำนักงานกองทุนสนับสนุนการวิจัย

(ความเห็นในรายงานนี้เป็นของผู้วิจัย สกอ.และสกว.ไม่จำเป็นต้องเห็นด้วยเสมอไป)

**Abstract**

In this research, Nanocrystalline Pt-Sn/$Al_2O_3$ catalysts with 0.3wt% Pt loading and 0.5-1.5 wt% Sn loading have been prepared by one-step flame spray pyrolysis (FSP) and conventional impregnation methods. The resulting nanopowders were characterized with X-ray diffraction, CO chemisorption, $N_2$-physisorption, X-ray photoelectron spectroscopy. Flame-made catalysts were composed of single-crystalline particles exhibiting the characteristic of γ-alumina with as-prepared primary particle size of 10 to 13 nm for 0.3wt.% Pt and Sn doping between 0.5 and 1.5 wt.%, respectively. Dehydrogenation reaction of propane to propene was used as the model reaction to investigate the catalytic properties of all catalysts. Flame-made catalysts exhibited the high activity and stability comparing with the impregnation one. These suggested changes in the catalytic properties when Pt and Sn were formed simultaneously in the support matrices by FSP method.

**Keywords** Flame Spray Pyrolysis, Pt-Sn/$Al_2O_3$, dehydrogenation, propane

**บทคัดย่อ**

ในงานวิจัยนี้ผลึกขนาดนาโนของตัวเร่งปฏิกิริยา Pt-Sn/$Al_2O_3$ ที่มีปริมาณโลหะแพลทินัม 0.3 เปอร์เซ็นต์โดยน้ำหนักและปริมาณโลหะดีบุก 0.5 ถึง 1.5 เปอร์เซ็นต์โดยน้ำหนักถูกเตรียมขึ้นในขั้นตอนเดียวโดยใช้เทคนิคเฟลมสเปรย์ไพโรไลซิส อนุภาคนาโนที่ได้ถูกนำไปศึกษาโดยอาศัยเทคนิควิเคราะห์การกระเจิงของรังสีเอ็กซ์ เทคนิคการวัดการดูดซับทางเคมีของแก๊สคาร์บอนมอนอกไซด์ เทคนิคการวัดการดูดซับทางกายภาพของแก๊สไนโตรเจน เทคนิคเอ็กซเรย์โฟโตอิเล็กตรอนสเปกโตรสโคปี ตัวเร่งปฏิกิริยาที่เตรียมจากเทคนิคเฟลมสเปรย์ไพโรไลซิสประกอบไปด้วยอนุภาคผลึกเดี่ยวของแกมมาอะลูมินาซึ่งมีขนาดเฉลี่ยอยู่ที่ 10 ถึง 13 นาโนเมตร สำหรับตัวเร่งปฏิกิริยา Pt-Sn/$Al_2O_3$ ที่มีปริมาณโลหะแพลทินัม 0.3 เปอร์เซ็นต์โดยน้ำหนักและปริมาณโลหะดีบุก 0.5 ถึง 1.5 เปอร์เซ็นต์โดยน้ำหนักตามลำดับ ปฏิกิริยาดีไฮโดรจิเนชันของโพรเพนถูกใช้เป็นปฏิกิริยาทดสอบสมบัติในการเป็นตัวเร่งปฏิกิริยาของตัวเร่งปฏิกิริยาที่เตรียมขึ้นทุกตัว ตัวเร่งปฏิกิริยาที่เตรียมจากเทคนิคเฟลมสเปรย์ไพโรไลซิสแสดงค่าความว่องไวในการเกิดปฏิกิริยาและค่าความเสถียรที่สูงเมื่อเปรียบเทียบกับตัวเร่งปฏิกิริยาที่เตรียมจากเทคนิคการเคลือบฝังแบบเดิม ผลที่ได้ชี้ให้เห็นว่าการเปลี่ยนแปลงของสมบัติในการเป็นตัวเร่งปฏิกิริยาของตัวเร่งปฏิกิริยาเมื่อโลหะแพลทินัมและโลหะดีบุกถูกทำให้เกิดขึ้นในโครงสร้างของตัวรองรับโดยใช้เทคนิคเฟลมสเปรย์ไพโรไลซิส

คำสำคัญ เฟลมสเปรย์ไพโรไลซิส Pt-Sn/$Al_2O_3$ ดีไฮโดรจิเนชัน โพรเพน

# Executive Summary

ในงานวิจัยนี้เราได้ทำการศึกษาการเตรียมผลึกขนาดนาโนของตัวเร่งปฏิกิริยา Pt-$Sn/Al_2O_3$ ที่มีปริมาณโลหะแพลทินัม 0.3 เปอร์เซ็นต์โดยน้ำหนักและศึกษาผลของปริมาณโลหะดีบุกที่เติมลงไปในช่วง 0.5 ถึง 1.5 เปอร์เซ็นต์โดยน้ำหนักในขั้นตอนเดียวด้วยเทคนิคเฟลมสเปรย์ไพโรไลซิส อนุภาคนาโนที่เตรียมขึ้นจะถูกนำไปศึกษาหาลักษณะทางเคมีและกายภาพโดยอาศัยเทคนิควิเคราะห์การกระเจิงของรังสีเอ็กซ์ เทคนิคการวัดการดูดซับทางเคมีของแก๊สคาร์บอนมอนอกไซด์ เทคนิคการวัดการดูดซับทางกายภาพของแก๊สไนโตรเจน เทคนิคเอ็กซเรย์โฟโตอิเล็กตรอนสเปกโตรสโคปี นอกจากนี้เรายังทดสอบสมบัติในการเป็นตัวเร่งปฏิกิริยาของตัวเร่งปฏิกิริยาที่เตรียมขึ้นทุกตัวด้วยปฏิกิริยาดีไฮโดรจิเนชันของโพรเพน และเพื่อเป็นการเปรียบเทียบสมบัติของตัวเร่งปฏิกิริยาที่เตรียมด้วยเทคนิคเฟลมสเปรย์ไพโรไลซิส เราได้ทาการเตรียมตัวเร่งปฏิกิริยา Pt-$Sn/Al_2O_3$ จากวิธีเคลือบฝังแบบแห้งอันเป็นวิธีทั่วไปในการเตรียมตัวเร่งปฏิกิริยาที่ใช้ในอุตสาหกรรมปัจจุบันเพื่อนำมาเปรียบเทียบกับ

ผลที่ได้พบว่าตัวเร่งปฏิกิริยาที่เตรียมจากเทคนิคเฟลมสเปรย์ไพโรไลซิสและที่เตรียมจากวิธีเคลือบฝังแบบแห้งบนตัวรองรับอะลมินาที่เตรียมจากเทคนิคเฟลมสเปรย์ไพโรไลซิสประกอบไปด้วยอนุภาคผลึกเดี่ยวของแกมมาอะลูมินาซึ่งมีขนาดเของอนุภาคเฉลี่ยอยู่ที่ 10 ถึง 13 นาโนเมตรสำหรับตัวเร่งปฏิกิริยา Pt-$Sn/Al_2O_3$ ที่มีปริมาณโลหะแพลทินัม 0.3 เปอร์เซ็นต์โดยน้ำหนักและปริมาณโลหะดีบุก 0.5 ถึง 1.5 เปอร์เซ็นต์โดยน้ำหนักตามลำดับ ในขณะที่ตัวเร่งปฏิกิริยาที่ถูกเตรียมจากวิธีเคลือบฝังแบบแห้งบนตัวรองรับอะลมินาทางการค้านั้นเราพบอนุภาคโลหะขนาดเล็กราว 2 ถึง 5 นาโนเมตรเกาะอยู่บนตัวรองรับอะลูมินาขนาดใหญ่ นอกจากนี้พบว่ารูพรุนของตัวเร่งปฏิกิริยาที่เตรียมจากเทคนิคเฟลมสเปรย์ไพโรไลซิสและที่เตรียมจากวิธีเคลือบฝังแบบแห้งบนตัวรองรับอะลมินาที่เตรียมจากเทคนิคเฟลมสเปรย์ไพโรไลซิสนั้นมีขนาดใหญ่กว่าตัวเร่งปฏิกิริยาที่ถูกเตรียมจากวิธีเคลือบฝังแบบแห้งบนตัวรองรับอะลมินาทางการค้า เมื่อนำตัวเร่งปฏิกิริยาที่เตรียมขึ้นมาทดสอบสมบัติในการเป็นตัวเร่งปฏิกิริยานั้นพบว่าตัวเร่งปฏิกิริยาที่เตรียมจากเทคนิคเฟลมสเปรย์ไพโรไลซิสแสดงค่าความว่องไวในการเกิดปฏิกิริยาและค่าความเสถียรที่สูงเมื่อเปรียบเทียบกับตัวเร่งปฏิกิริยาที่เตรียมจากเทคนิคการเคลือบฝังแบบเดิม ผลที่ได้สามารถอธิบายได้จากขนาดรูพรุนที่สูงกว่าและการฟอร์มตัวเป็นอัลลอยด์ระหว่างโลหะแพลทินัมและโลหะดีบุกในโครงสร้างของตัวรองรับโดยใช้เทคนิคเฟลมสเปรย์ไพโรไลซิส

# Chapter I

## Introduction

Due to the uncertain oil price and growing demand of propylene in the past few years, the catalytic dehydrogenation of propane from natural gas has received much attention as an alternative way for producing propylene. The dehydrogenation of propane is an endothermic reaction that requires high temperature, which promotes the thermal cracking reaction to coke and light alkane. To overcome this problem, new catalysts with high-activity, high-stability and high-selectivity are required. The most widely studied are chromium- and platinum-based catalysts have been studied widely [1]. However, both of them have relatively poor reaction stability due to the carbon deposits.

Addition of Sn to Pt-based catalysts is well known to promote desired dehydrogenation reactions and inhibit coking reactions [2]. Improvement on catalyst activity and stability by Sn doping has been reported by many researchers [3, 4, 5, 6, 7]. The role of Sn in PtSn catalyst has been explained in terms of geometric effect and/or electronic effect. For geometric effect, tin decreases the size of platinum ensembles, which reducing hydrogenolysis and coking reactions, while for electronic effect, tin modifies the electronic density of Pt, either due to a positive charge transfer from $Sn^{n+}$ species or to the different electronic structures of PtSn alloys. This modification may be responsible for changes in the heat of adsorption of different adsorbates participating in the reaction

Bimetallic Pt and Sn supported on different supports such as metal oxides ($Al_2O_3$, $ZrO_2$, $SiO_2$, $TiO_2$) [2, 3, 8, 9, 10], zeolites (ZSM-5) [11, 12], and mesoporous

materials (SBA-15) [13], which are believed to be the promising catalysts for propane dehydrogenation have been extensively investigated. Among those, Pt-Sn/$Al_2O_3$ is one of the most favorite dehydrogenation catalysts, owing to the strong interaction between Pt metal and $Al_2O_3$ supports, which could affect reduction behavior and stability of the catalyst.

Flame synthesis, especially flame spray pyrolysis (FSP), is a relatively new process for one-step synthesis of supported metal catalysts. It is generally known as a method for making nanoparticles such as fume silica, titania, and carbon black in large quantity at low cost [14]. The applications of supported metal catalysts synthesized via one-step flame spray pyrolysis have been reported continuously. For examples, flame-made Pt-Ba/$Al_2O_3$ and Pt/Ba/$Ce_xZr_{1-x}O_2$ have been investigated in lean-$NO_x$ storage-reduction [15-16]. High surface area Ag/ZnO prepared by flame spray pyrolysis has been reported to exhibit high photocatalytic performance in UV-photodegradation of methylene blue [17]. Baiker et al. [18-20] successfully applied the flame spray pyrolysis method for synthesis of various $Al_2O_3$ supported noble metal catalysts. The flame-made Pt/$Al_2O_3$ showed an improved turnover frequency in the hydrogenation of ethyl pyruvate compared to a conventional porous catalyst and Pd/$Al_2O_3$ was tested in enantioselective hydrogenation of 4-methoxy-6-methyl-2-pyrone. Our recent studies also show that the flame-made Pd/$SiO_2$ exhibited the high turnover frequency in the selective hydrogenation of heptyne to heptene comparing with impregnation one. The structural differences of the flame-made and conventionally prepared catalysts have often been explained as the reasons for their differences in catalytic behaviors [21-22].

In this work, Pt-Sn/$Al_2O_3$ catalysts with 0.3wt% Pt and 0.5-1.5 wt% Sn loadings were prepared in one-step by flame spray pyrolysis. The catalysts were

characterized by $N_2$ physisorption, X-ray diffraction (XRD), CO pulse chemisorption, transmission electron spectroscopy (TEM), and X-ray photoelectron spectroscopy (XPS). The catalytic behaviors of the flame-made Pt-Sn/$Al_2O_3$ were evaluated in the dehydrogenation of propane. Pt-Sn/$Al_2O_3$ prepared by conventional impregnation of Pt and Sn precursors on both flame-synthesized and commercial $Al_2O_3$ were employed for comparison purposes. The stronger metal-support interaction in the flame-made catalyst is believed to produce great beneficial effect in such reaction.

# Chapter II

# EXPERIMENTAL

## 2.1 Catalyst Preparations

### *Preparation of flame-made catalyst*

Syntheses Pt-Sn/$Al_2O_3$ catalyst was carried out using a spray flame reactor. Platinum actetylacetonate, tin ethylhexanoate, and aluminum tri-sec-butoxide from Aldrich were used as platinum, tin, potassium zinc and aluminum precursors, respectively. Precursors were prepared by dissolving the designed amounts of metal precursor in xylene (MERCK; 99.8 vol%). The total metal concentration was maintained at 0.3 M. The platinum concentration was fixed at 0.3 wt%, while the tin contents were ranged between 0.5 and 1.5 wt%. Using a syringe pump, 5 ml/min of precursor solution was dispersed into fine droplets by a gas-assist nozzle fed by 5 l/min of oxygen (Thai Industrial Gas Limited; purity > 99%). The pressure drop at the capillary tip was maintained at 1.5 bar by adjusting the orifice gap area at the nozzle. The spray was ignited by supporting flamelets fed with oxygen (3 l/min) and methane (1.5 l/min) which are positioned in a ring around the nozzle outlet. A sintered metal plate ring (8 mm wide, starting at a radius of 8 mm) provided additional 10 l/min of oxygen as sheath for the supporting flame. The product particles were collected on a glass fiber filter (Whatman GF/C, 15 cm in diameter) with the aid of a vacuum pump.

### *Preparation of impregnated-made catalyst*

To compare the activity of flame-made catalyst, the bi-and tri-metallic catalysts were prepared by incipient wetness impregnation, using organic solutions of platinum actetylacetonate, tin ethylhexanoate, in xylene. The incipient wetness impregnation procedure is as follow:

1) The PtSn catalyst was prepared by co-impregnation. The metal contents in the catalysts were 0.3wt% for Pt, and 1wt% for Sn. A

commercial (JRC-AlO2) and flame-made $Al_2O_3$ were used as the catalyst support.

2) Both aluminas were impregnated with the droplet of metal solution.

3) The obtained powder was dried in air at 110$^{o}$C overnight and then calcined at 550$^{o}$C in air for 3 hour

## 2.2 Catalyst Characterization

To investigate the physiochemical properties of catalysts, fresh and spent catalysts was characterized by several techniques

### 1. $N_2$-physisorption

The BET (Brunauer Emmett Teller) surface area, average pore size diameters, and pore size distribution are obtained from nitrogen adsorption/desorption isotherms determined at liquid nitrogen temperature on an automatic analyzer using Micromeritics ASAP 2020 (surface area and porosity analyzer).

### 2. X-ray Diffraction (XRD)

The bulk crystal structure and chemical phase composition are determined by diffraction of an X-ray beam as a function of the angle of the incident beam. The XRD spectrum of the catalyst is measured by using a SIEMENS D500 X-ray diffractometer and Cu $K_{\alpha}$ radiation. The crystallite size is calculated from Scherrer's equation.

### 3. Transmission Electron Microscopy (TEM)

The morphology, particle size and particle distribution will be observed using JEOL-JEM 200CX transmission electron microscope operated at 100 kV.

### 4. CO-pulse chemisorptions

The active sites and relative percentages dispersion of platinum catalyst were determined by CO-pulse chemisorption technique using a Micromeritics ChemiSorb 2750 system attached with ChemiSoft TPx software at room temperature.

### 5. X-ray Photoelectron Spectroscopy (XPS)

XPS analysis was performed using an AMICUS photoelectron spectrometer equipped with a Mg $K_\alpha$ X-ray as a primary excitation and a KRATOS VISION2 software. XPS elemental spectra were acquired with 0.1 eV energy step at a pass energy of 75 kV. The C 1s line was taken as an internal standard at 285.0 eV.

### 6. Thermal Gravimetric and Differential Temperature Analysis (TG/DTA)

Amount of coke deposited on the surface of catalyst were detected by Thermal gravimetric and differential temperature analysis (TG/DTA) using an SDT Analyzer Model Q600 from TA Instruments, USA

## 2.3 Catalytic Evaluation

The dehydrogenation of propane (Thai Industrial Gas) was carried out in a fixed-bed reactor with an inner diameter 6 mm. Aprroximately 0.1 g of catalyst was loaded in the middle of reactor. Prior to the experiments the catalysts were pretreated in flowing $H_2$ (30 ml/min) at 773 K for 1 h. The reaction was carried out isothermally at 823 K and at atmospheric pressure. The reaction mixture composed of $H_2$, $C_3H_8$ and Ar ($H_2/C_3H_8$/Ar molar ratio = 1:1:5) was fed to the reactor with the weight hourly space velocity (WHSV) based on propane of 5 $h^{-1}$. A purge gas (Ar) flow of 30 ml/min was used and the reaction mixture was preheated at 773 K. The product gases were analyzed on-line using a gas chromatograph with a TCD detector using SUS Column PorapakQ, 80/100 mesh column.

# CHAPTER 3

# Results and Discussion

## 3.1 Catalyst Properties

**Figure 3.1** shows the XRD patterns of impregnation- and flame-made $Pt/Al_2O_3$ and $Pt\text{-}Sn/Al_2O_3$ catalysts with Sn loadings 0.5-1.5 wt%. All the catalyst samples exhibited only the characteristic peaks of $\gamma\text{-}Al_2O_3$ where additional peaks corresponding to Pt, Sn, and other alumina phases were not observed due probably to the low amount of Pt and Sn present and/or high dispersion of these metals on the $Al_2O_3$ supports. It is also indicated that addition of Pt or Sn simultaneously with Al during flame synthesis did not affect alumina phase transformation. Formation of γ-phase in high temperature flame can be explained by the fact that the particles spent only few second in the flame. This result is consistence with the work from Baiker et al. [18-20].

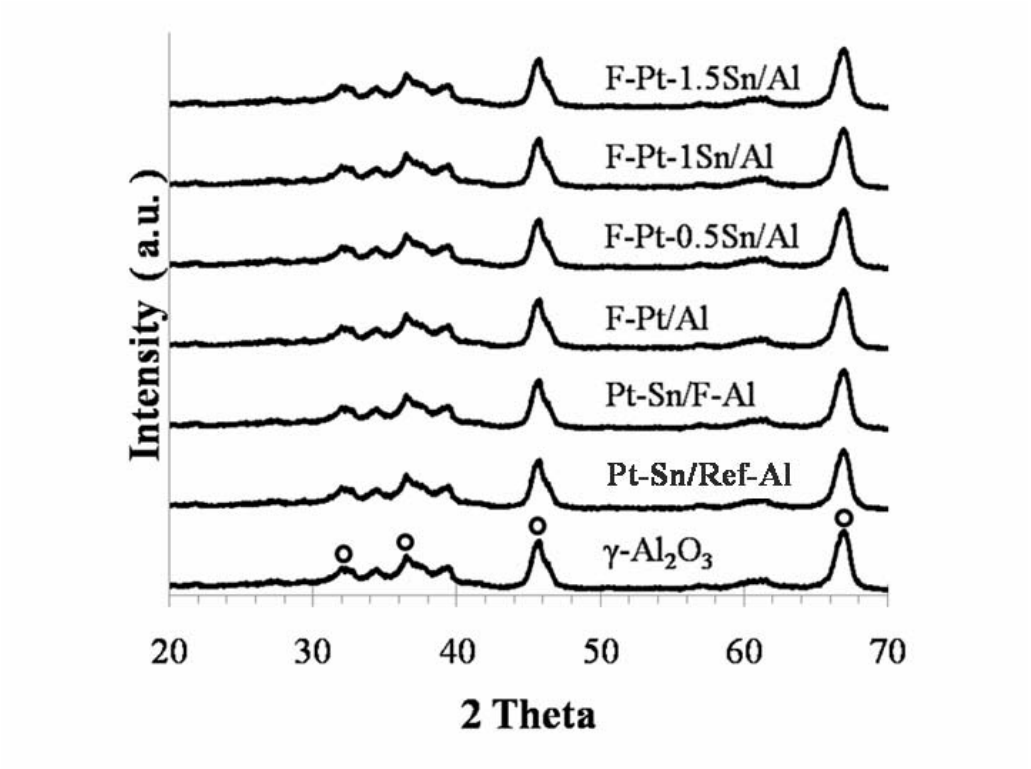


**Figure 3.1** XRD patterns of the flame-made Pt-Sn/Al2O3 catalysts (as synthesized).

**Figure 3.2** shows typical TEM micrographs of the impregnated and flame-made $Pt/Al_2O_3$ and $Pt\text{-}Sn/Al_2O_3$ catalysts. The impregnation-made PtSn supported on commercial $Al_2O_3$ catalysts (Pt-1.0Sn/Com-Al) consisted of agglomerated large particles of alumina and spherical Pt/PtO nanoparticles/clusters with average size between 2 to 5 nm dispersed on alumina surface as dark spots. The flame-made powder consisted of spherical primary particles with average size around 7 to 18 nm. Pt/PtO metal clusters were not distinguishable for both the impregnation-made Pt-Sn on flame-made $Al_2O_3$ support (Pt-1.0Sn/F-Al) and all the flame-made catalyts due to poor contrast between the Pt, Sn and Al atoms in TEM images.

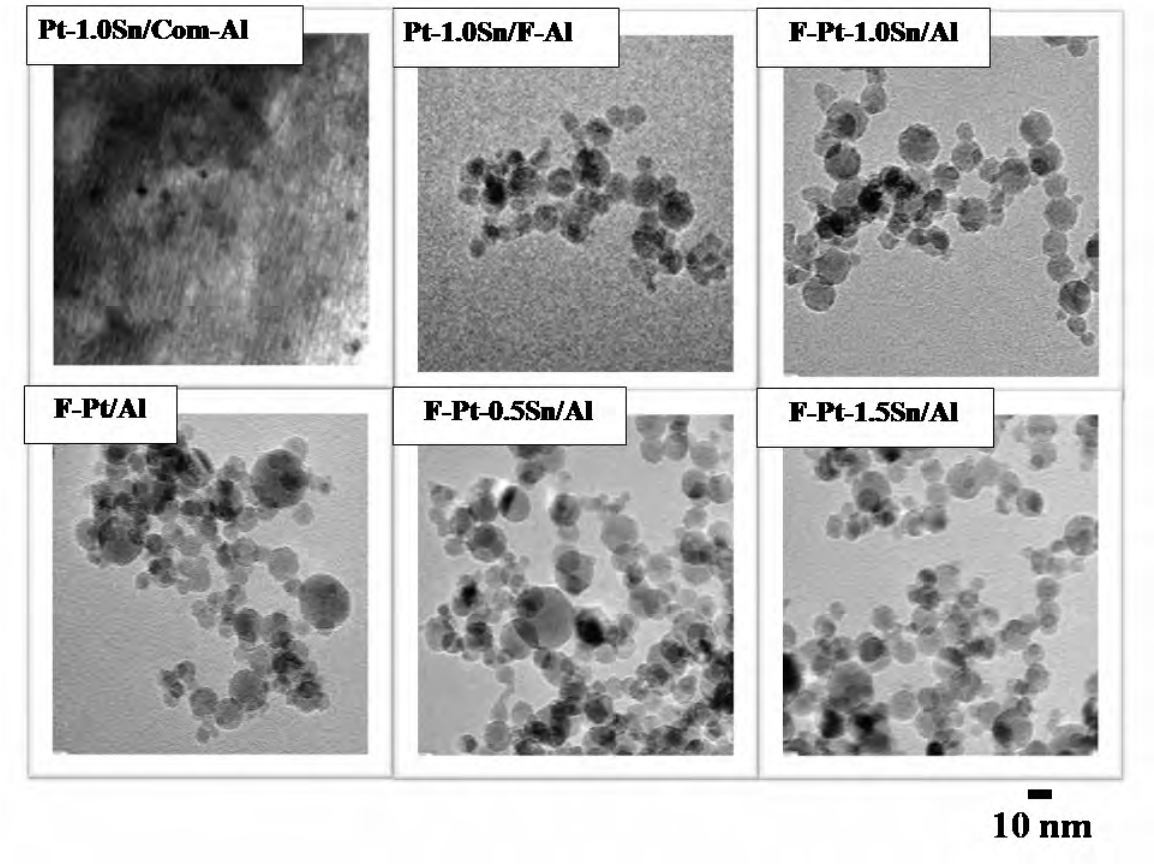


**Figure 3.2** TEM micrographs of the various flame- and impregnation-made Pt-Sn/$Al_2O_3$ catalysts

**Figure 3.3** shows the XRD particle size ($d_{XRD}$) for $Al_2O_3$ (triangles), the BET equivalent particle size ($d_{BET}$; circles) and average particle size obtained from TEM analysis ($d_{TEM}$; square), as a function of Sn loading for the flame-made Pt-Sn/$Al_2O_3$ powders. The calculated $d_{BET}$ data were found to be in good agreement with the $d_{XRD}$ and $d_{TEM}$ values indicating that the particles were single crystalline with average particle size between 9-13 nm. **Table 1** summarizes physicochemical properties of the impregnated and flame-made Pt-Sn/$Al_2O_3$ catalysts. The BET surface areas of the commercial and flame-made $Al_2O_3$ supports were 145 and 105 $m^2/g$, respectively whereas those of the corresponding impregnation-made Pt-Sn/$Al_2O_3$ catalysts were 139 and 103 $m^2/g$. Small decrease on BET surface area can be explained pore

blockage of platinum and tin oxide clusters during impregnation. The BET surface areas of flame-made catalysts were ranged between 112 and 122 $m^2/g$. An increase in BET surface area of the flame-made Pt-Sn/$Al_2O_3$ catalysts compared to the flame-made $Al_2O_3$ support was due probably to inhibition of the growth of the $Al_2O_3$ particles by Pt and Sn dopant. Such result is similar to our earlier works [23] for Pd/$SiO_2$ nanoparticles prepared by flame spray pyrolysis that adding metal particles resulted in an increase in BET surface area of the $SiO_2$ support. From $N_2$ adsorption results, The FSP- and impregnation-made catalysts supported on flame-made $Al_2O_3$ catalysts are nonporous, whereas the impregnation-made catalysts supported on commercial one is a mesoporous material.

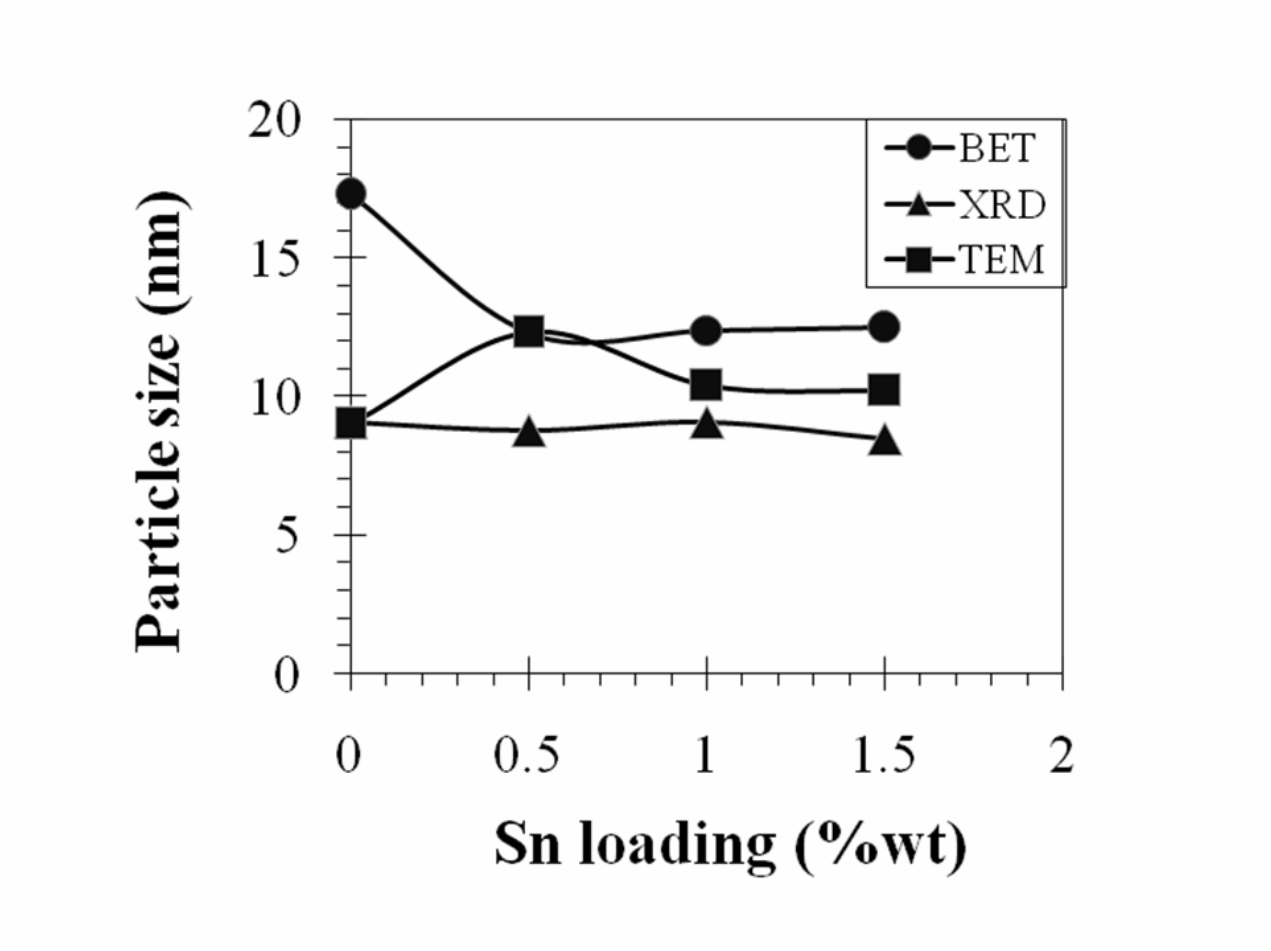

**Figure 3** XRD particle size ($d_{XRD}$) for $Al_2O_3$ (triangles), together with the BET equivalent particle size ($d_{BET}$; circles) and TEM particle size ($d_{TEM}$; square), as a function of Sn loading for Pt-Sn/$Al_2O_3$ powders.

The relative amounts of active surface Pt metal on the catalyst samples were calculated from CO chemisorption experiments at room temperature. The calculation of Pt active sites was based on the assumption that one carbon monoxide molecule adsorbs on one platinum site. The Pt active sites were found to decrease from $2.3x10^{18}$ to $1x10^{18}$ sites/g-catalyst as the Sn contents increased from 0 to 1.5 wt% and corresponding to decreasing of %Pt metal dispersion from 28 to 12.2%. This decrease can be due to the formation of Pt–Sn ensembles or alloys that do not adsorb CO [24]. Comparing between the preparation methods, Pt active size decreases in the order of Pt-1.0Sn/F-Al > Pt-1.0Sn/Com-Al > F-Pt-1.0Sn/Al. The average $Pt^0$ metal particle sizes calculated from CO chemisorption were in the range of 4 to 9 nm.

Formation of Pt-Sn/$Al_2O_3$ nanoparticles by flame spray pyrolysis was considered as follows: the sprayed droplets of precursor solution were evaporated and combusted as soon as they met the flame at very high temperature and released the metal atoms, then nucleation and growth of particles by coagulation and condensation occurred along the axial direction of the flame. Comparing to alumina, the vapor pressure of Pt/PtO was much higher in the hot flame environment, and consequently $Al_2O_3$ particle formation started earlier. Further downstream the flame, at lower temperatures, Pt/PtO started to form small particles and/or deposits directly on the $Al_2O_3$ support. However, since the process occurred in a very high temperature environment, it was possible that some of the metal particles were covered by support

matrix. Similar particle formation mechanism has been suggested for flame-made $Pd/Al_2O_3$ and $Pt/TiO_2$ [15,25].

X-ray photoelectron spectroscopy is a powerful tool for determination of the surface compositions of the catalysts and the interaction between Pt, Sn and alumina supports. The elemental scans of the various flame- and impregnation-made Pt-$Sn/Al_2O_3$ catalysts are summarized in **Table 3.1**. It was found that the Pt peak was not observed in all samples, which due probably to low amount of Pt. The XPS peak for Sn was observed at around 488 eV for impregnation-made Pt-$Sn/Al_2O_3$ catalysts, while the flame-made catalysts exhibited the characteristic peak corresponding to oxidized Sn species at around 486 eV. According to literature data, the line corresponding to Sn $3d_{5/2}$ for $Sn^{2+}$ has a binding energy at 486.5–486.9 eV, while the Sn $3d_{5/2}$ line for $Sn^{4+}$ has a binding energy at 486.5-488 eV [26, 27, 28]. A small shift to the lower binding energies of the flame-made catalysts suggests that more reducible form of Sn was formed by flame synthesis. The Sn/Al atomic ratios of all the catalysts are also given in Table 1. It was found that this value for PtSn/Com-Al was ten and twenty-five times higher than PtSn/F-Al and F-PtSn/Al, respectively. Such result could be attributed to the larger average pore size of the flame-made catalyst, which made the impregnated Pt and Sn molecule located deeper inside the pores. In contrast, Pt and Sn particles on the FSP-made catalysts may be surrounded by support matrix i.e., in the form of Al-O group resulting in much lower Sn/Al ratio. Such phenomena could also explain the inhibition of CO chemisorption on the flame-made catalysts. Moreover, it is likely that the interaction between Pt, Sn species, and $Al_2O_3$ support in the flame-synthesized catalysts was stronger than to those prepared by conventional impregnation which also reduced the chemisorption of CO molecules.

**Table 3.1** Physicochemical Properties of Flame- and impregnation-made $Al_2O_3$ and Pt-Sn/$Al_2O_3$ Catalysts

| Catalyst | BET Surface Areas ($m^2/g$) | Total pore Volume (cc/g) | Average Pore diameter (nm) | CO Chemisorption Results | | | XPS B.E. (eV) Sn $3d_{5/2}$ | Atomic ratio Sn/Al |
|---|---|---|---|---|---|---|---|---|
| | | | | CO uptake (molecule CO/g cat.) | %Pt dispersion | $d_P$ $Pt^0$ (nm) | | |
| $Al_2O_3$ (Com) | 145 | 0.29 | 13.1 | n/a | n/a | n/a | n/a | n/a |
| $Al_2O_3$ (FSP) | 104 | 0.42 | 64.2 | n/a | n/a | n/a | n/a | n/a |
| Pt-1.0Sn/Com-Al | 139 | 0.26 | 9.2 | $1.44x10^{18}$ | 17.3 | 6.2 | 488.3 | 0.131 |
| Pt-1.0Sn/F-Al | 103 | 0.29 | 50.9 | $1.95x10^{18}$ | 23.4 | 4.6 | 488.4 | 0.013 |
| F-Pt/Al | 110 | 0.37 | 63.7 | $2.32x10^{18}$ | 28.0 | 3.9 | n/a | n/a |
| F-Pt-0.5Sn/Al | 122 | 0.36 | 63.5 | $1.75x10^{18}$ | 21.0 | 5.1 | 486.1 | 0.002 |
| F-Pt-1.0Sn/Al | 112 | 0.31 | 59.2 | $1.22x10^{18}$ | 14.6 | 7.4 | 486.7 | 0.005 |
| F-Pt-1.5Sn/Al | 120 | 0.31 | 56 | $1.01x10^{18}$ | 12.2 | 8.8 | 486.5 | 0.010 |

*3.2 Dehydrogenation of propane*

The catalytic behavior of the flame-made $Pt/Al_2O_3$ and $Pt\text{-}Sn/Al_2O_3$catalysts was investigated in the dehydrogenation of propane reaction. The catalytic performance in terms of propane conversions and selectivity to propene and the turnover frequencies calculated based on CO chemisorption results of the flame-made $Pt/Al_2O_3$ and $Pt\text{-}Sn/Al_2O_3$catalysts are given in **Table 3.2**. The results were also compared to the impregnated Pt-Sn supported on flame-made and commercial $Al_2O_3$ supports. The conversion of propane for the flame-made $Pt/Al_2O_3$ and $Pt\text{-}Sn/Al_2O_3$catalysts increased from 7.3 to 22.6% as Sn loading increased from 0 to 0.5wt% and decreased to 12.7% when Sn loading was increased further to 1.5 wt%. When comparing between preparation methods, the propane conversion was improved in order of flame-made $Pt\text{-}Sn/Al_2O_3$ > impregnation-made Pt-Sn/flame-made $Al_2O_3$ > impregnation-made Pt-Sn/com-$Al_2O_3$.

**Table3. 2** Catalytic Properties for propane dehydrogenation

| Catalyst | % Conversion | | $\%C_3H_6$ selectivity | TOFs ($s^{-1}$) [a] |
|---|---|---|---|---|
| | Initial | Final | | |
| Pt-1.0Sn/Com-Al | 6.6 | 5.1 | 97 | 0.9 |
| Pt-1.0Sn/F-Al | 25.3 | 15.1 | 97 | 2.6 |
| F-Pt/Al | 11.8 | 7.3 | 98 | 1.1 |
| F-Pt-0.5Sn/Al | 33.8 | 22.6 | 99 | 3.7 |
| F-Pt-1Sn/Al | 29.1 | 17.8 | 97 | 4.7 |
| F-Pt-1.5Sn/Al | 18.8 | 12.6 | 98 | 3.5 |

[a] TOF = mole product/mole Pt metal/s (based on CO chemisorption results).

The plot between propane conversion and reaction time are shown in **Figure 3.4**. The selectivity for propene was in the range of 96 to 99% for all the $Pt/Al_2O_3$ and $Pt-Sn/Al_2O_3$catalysts. The specific activities of the flame-made catalysts are also expressed in terms of turnover frequency (TOF) which is defined as mole of product/mole of metal/time. Plot between TOFs of all $Pt-Sn/Al_2O_3$ catalysts is shown in **Figure 3.5**. Comparing between the preparation methods, TOFs of the flame-made $Pt-Sn/Al_2O_3$ catalysts improved in the order of F-Pt-1Sn/Al > F-Pt-0.5Sn/Al ~ F-Pt-1.5/Al > F-Pt/Al. For a similar Sn loading, TOFs of the flame-made catalyst were nearly two times higher than those of the impregnation-made catalysts supported on both flame-made and commercial alumina supports. The better catalytic performance of the flame-made catalysts can be explained by the different pore structure of the prepared catalysts, the location of Pt and Sn on alumina support, and the interaction between Pt-Sn and $Al_2O_3$.

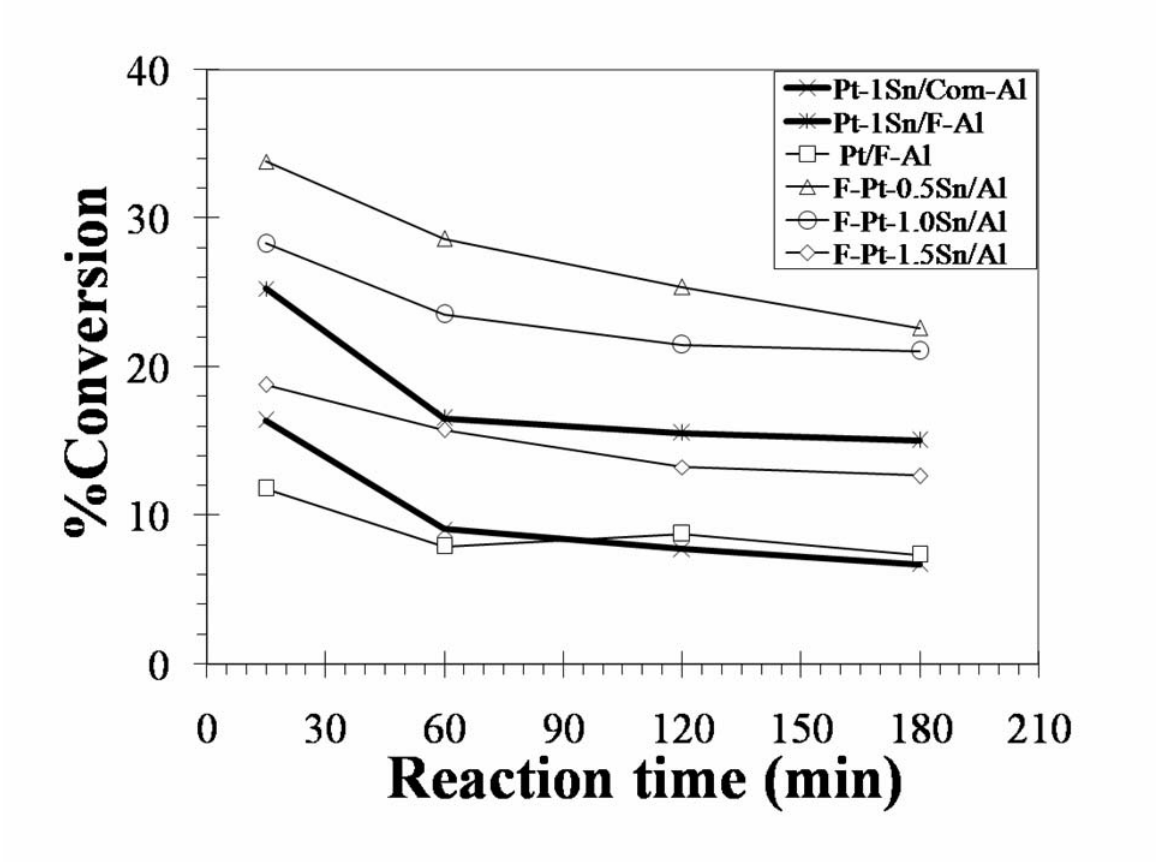


**Figure 3.4** Plot between propane conversion and reaction time of all catalysts

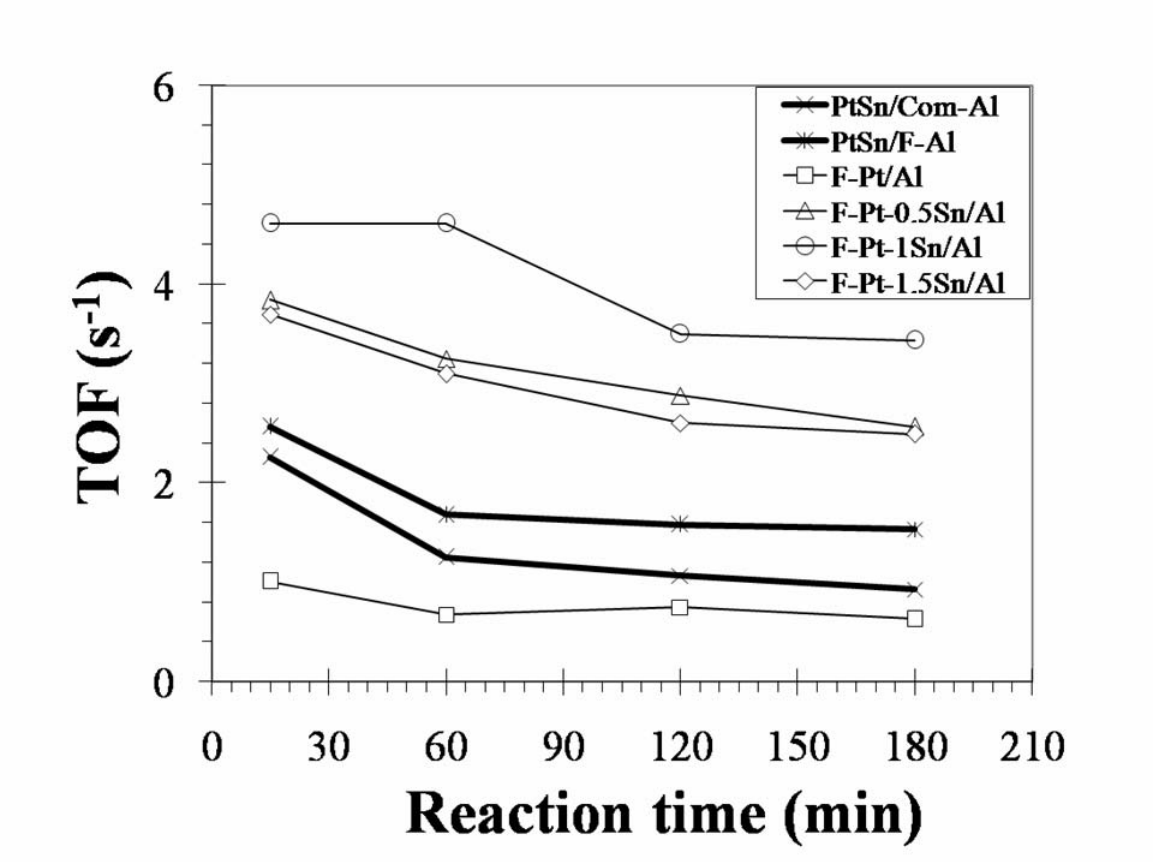


**Figure 5** Plot between TOFs and Sn contents reaction time of all catalysts

Deactivation performances of flame- and impregnation-made catalysts are shown in **Figure 3.6**. Compared to the conventional impregnation method, the flame-made catalyst exhibited the highest stability due probably to their larger pore size resulting in lower amount of carbon blocking active sites. Considering the effect of Sn content, %deactivation decreased from 37.5 to 25% as Sn loading increased from 0 to 1 wt% and then decreased to 32.5% after Sn loading further increased to 1.5%. Such results revealed that addition of a suitable amount of Sn is required in order to improve activity and stability of the catalysts. An opposite effect was observed with the excessive amount of Sn loading. Due to the fact that there are two active centers (metal and acid sites) for the

dehydrogenation reaction and there exists an optimum ratio between the number of acid sites and the number of metal sites of catalysts, adding of an appropriate amount of Sn would adjust the ratio between these two sites. However, when the concentration of Sn further increased, larger amount of $Sn^0$ species could be produced and resulted in an alloy formation, thus catalyst activity decreased.

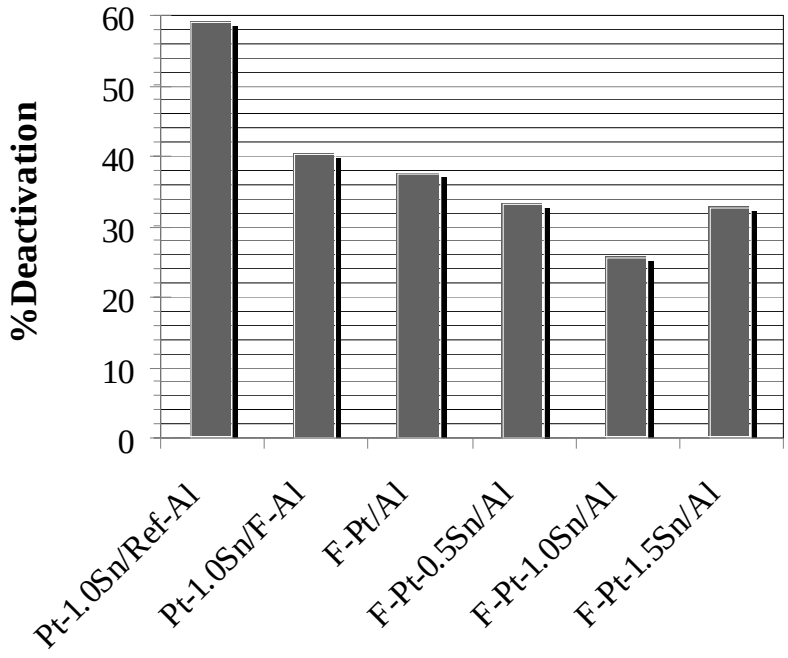


**Figure 3.6** Percentages of the catalyst activity change for flame- and impregnation-made catalysts

# Chapter IV

## Conclusions

The Pt-Sn/$Al_2O_3$ catalysts synthesized by one-step flame spray pyrolysis have shown very high catalytic activity and stability for dehydrogenation of propane. The resulting catalysts consisted of single-crystalline particles exhibiting the characteristic of γ-alumina with average primary particle size of 10 to 13 nm. Flame-made catalyst exhibited the good catalytic activity with very high propene selectivity (>97%) comparing with impregnation-made one. TOFs of the flame-made catalysts were two times higher than the impregnation-made catalysts. These higher catalytic activity and stability of flame-made catalyst can be correlated to the nature of pore structure and interaction between Pt–Sn-support.

## Output ที่ได้จากโครงการ

งานวิจัยนี้ได้เริ่มดำเนินงานตั้งแต่ประมาณเดือน มิ.ย. 2551 สิ้นสุดโครงการ มิ.ย. 2553 รวมระยะเวลาดำเนินงาน 2 ปี ผลที่ได้รับจากงานวิจัย ได้แก่

1. สามารถสังเคราะห์ตัวเร่งปฏิกิริยาขนาดนาโนของแพลทินัม-ทินที่อยู่บนตัวรองรับอะลูมินาขึ้นได้ในขั้นตอนเดียวด้วยเทคนิคเฟลมสเปรย์ไพโรไลซิส
2. การศึกษาการประยุกต์ใช้ตัวเร่งปฏิกิริยาดังกล่าวในปฏิกิริยาดีไฮโดรจิเนชันของโพรเพน พบว่ามีประสิทธิภาพสูงกว่าตัวเร่งปฏิกิริยาที่เตรียมขึ้นจากวิธีเดิมรวมถึงตัวเร่งปฏิกิริยาที่มีขายในท้องตลาด
3. นอกจากนี้พบว่าคุณลักษณะและประสิทธิภาพของตัวเร่งปฏิกิริยาที่ดีขึ้นของตัวเร่งปฏิกิริยาเตรียมด้วยเทคนิคเฟลมสเปรย์ไพโรไลซิสเกิดจากขนาดรูพรุนของตัวรองรับตัวเร่งปฏิกิริยาที่สูงขึ้นและการเกิดการฟอร์มตัวของแพลทินัม-ทินอัลลอยด์

- ได้เสนอผลงานเพื่อตีพิมพ์ในวารสารที่มี Peer review ระดับนานาชาติจำนวน 2 บทความ โดย 2 บทความได้รับการตีพิมพ์เรียบร้อยแล้ว และอีก 1 ผลงานกำลังอยู่ในระหว่างการเตรียมบทความ

**ผลงานที่ได้รับการตีพิมพ์ในวารสารที่มี Peer review ระดับนานาชาติ**

1) S. Pisduangdaw, J. Panpranot, C. Methastidsook, C. Chaisuk, K. Faungnawakij, P. Praserthdam, and **O. Mekasuwandumrong** "Characteristics and Catalytic Properties of Pt-Sn/$Al_2O_3$ Nanoparticles Synthesized by One-Step Flame Spray Pyrolysis in the Dehydrogenation of Propane" Applied Catalysis A .General 370 (2009) 1-6.

# ภาคผนวก

1) Reprint of the paper entitled ““Characteristics and Catalytic Properties of Pt-Sn/$Al_2O_3$ Nanoparticles Synthesized by One-Step Flame Spray Pyrolysis in the Dehydrogenation of Propane” Applied Catalysis A .General 370 (2009) 1-6.

## Reference

[1] M.M. Bhasin, J.H. McCain, B.V. Vora, T. Imai, P.R. Pujado, Applied Catalysis A: General 221 (2001) 397.

[2] P. Praserthdam, N. Grisdanurak, W. Yuangsawatdikul, Chemical Engineering Journal 77 (2000) 215.

[3] O. A. Bariås, A. Holmen, and E. A. Blekkan, Journal of Catalysis 158 (1996) 1.

[4] S. B. Kogan, H. Schramm, M. Herskowitz, Applied Catalysis A: General 208 (2001) 185

[5] J. Salmones, J. Wang, J. A. Galicia, G. Aguilar-Rios, Journal of Molecular Catalysis A: Chemical 184 (2002) 203

[6] L. Bednarova, C. E. Lyman, E. Rytter, and A. Holmen, Journal of Catalysis 211 (2002) 335

[7] M. Larsson, M. Hultén, E. A. Blekkan, and B. Andersson, Journal of Catalysis 164 (1996) 44.

[8] S. B. Kogan, H. Schramm, M. Herskowitz, Studies in Surface Science and Catalysis 88 (1994) 519-524.

[9] C. Larese, J. M. Campos-Martin, J. J. Calvino, G. Blanco, J. L. G. Fierro, and Z. C. Kang, Journal of Catalysis 208 (2002) 467-478.

[10] A. Vázquez-Zaval, A. Ostoa-Montes, D. Acosta, A. Gómez-Cortés, Applied Surface Science 136 (1998) 62-72.

[11] Y. Zhang, Y. Zhou, A. Qiu, Y. Wang, Y. Xu, P. Wu, Catalysis Communications 7 (2006) 860-866.

[12] Y. Zhang, Y. Zhou, K. Yang, Y. Li, Y. Wang, Y. Xu, P. Wu, Microporous and Mesoporous Materials 96 (2006) 245-254.

[13] L. Huang, B. Xu, L. Yang, Y. Fan, Catalysis Communications 9 (2008) 2593-2597.

[14] W. J. Stark , S. E. Pratsinis, Powder Technology 126 (2002) 103.

[15] M. Piacentini, R. Strobel, M. Maciejewski, S. E. Pratsinis, and A. Baiker, J. Catal. 243 (2006) 43.

[16] R. Strobel, F. Krumeich, S. E. Pratsinis, and A. Baiker, J. Catal. 243 (2006) 229.

[17] M. J. Height, S. E. Pratsinis, O. Mekasuwandunrong, and P. Praserthdam, Appl. Catal. B 63 (2006) 305.

[18] R. Strobel, W. J. Stark, L. Madler, S. E. Pratsinis, and A. Baiker, J. Catal. 213 (2003) 296.

[19] R. Strobel, F. Krumeich, W. J. Stark, S. E. Pratsinis, and A. Baiker, J. Catal. 222 (2004) 307.

[20] S. Hannemann, J.-D. Grunwaldt, P. Lienemann, D. Gunther, F. Krumeich, S. E. Pratsinis, and A. Baiker, Appl. Catal. A 316 (2007) 226.

[21] S. Somboonthanakij, O. Mekasuwandumrong, J. Panpranot, T. Nimmanwudtipong, R. Strobel, S.E. Pratsinis, and P. Praserthdam, Catalysis Letters 119 (2007) 346.

[22] O. Mekasuwandumrong, S. Somboonthanakij, P. Praserthdam and J. Panpranot, Industrial & Engineering Chemistry Research 48 (2009) 2819.

[23] S. Hannemann, J. Grunwaldt, F. Krumeich, P. Kappen A. Baiker, Applied Surface Science 252 (2006) 7862.

[24] S. M. Stagg, C. A. Querini, W. E. Alvarez, D. E. Resasco, Journal of Catalysis, 168 (1997) 75.

[25] W. Y. Teoh, L. Mädler, D. Beydoun, S. E. Pratsinis and R. Amal, Chemical Engineering Science, 60 (2005) 5852.

[26] Homs, J. Llorca, M. Riera, J. Jolis, J. Fierro, J. Sales and P. Ramírez de la Piscina, J. Mol. Catal. A: Chem. 200 (2003) 251.

[27] A. Huidobro, A. Sepúlveda-Escribano and F. Rodríguez-Reinoso, Journal of Catalysis 212 (2002) 94.

[28] E. Merlen, P. Beccat, J.C. Bertolini, P. Delichere, N. Zanier and B. Didillon, Journal of Catalysis 159 (1996)178.

Applied Catalysis A: General 370 (2009) 1–6

Contents lists available at ScienceDirect

Applied Catalysis A: General

journal homepage: www.elsevier.com/locate/apcata

# Characteristics and catalytic properties of Pt–Sn/$Al_2O_3$ nanoparticles synthesized by one-step flame spray pyrolysis in the dehydrogenation of propane

Sukanya Pisduangdaw [a], Joongjai Panpranot [b], Chatthip Methastidsook [a], Choowong Chaisuk [a], Kajornsak Faungnawakij [c], Piyasan Praserthdam [b], Okorn Mekasuwandumrong [a,*]

[a] Department of Chemical Engineering, Faculty of Engineering and Industrial Technology, Silpakorn University, Nakorn Pathom 73000, Thailand
[b] Center of Excellence on Catalysis and Catalytic Reaction Engineering, Department of Chemical Engineering, Faculty of Engineering, Chulalongkorn University, Bangkok 10330, Thailand
[c] National Nanotechnology Center, National Science and Technology Development Agency (NSTDA), 111 Thailand Science Park, Paholyothin Rd., Patumthani 12120, Thailand

ARTICLE INFO

*Article history:*
Received 28 April 2009
Received in revised form 29 July 2009
Accepted 6 August 2009
Available online 13 August 2009

*Keywords:*
Flame spray pyrolysis
Pt–Sn/$Al_2O_3$
Dehydrogenation
Propane

ABSTRACT

The Pt–Sn/$Al_2O_3$ catalysts with 0.3 wt% Pt and 0.5–1.5 wt% Sn loading were prepared by one-step flame spray pyrolysis (FSP). Unlike the catalysts prepared by conventional impregnation method, the FSP-derived catalysts were composed of single-crystalline γ-alumina particles with the as-prepared primary particle size of 10–18 nm and contained only large pores. The FSP catalysts exhibited superior catalytic activity and better stability than the ones made by impregnation in the dehydrogenation of propane, while they did not alter the selectivity to propylene (in all cases, propylene selectivity ≥96%). The presence of large pores in the flame-made catalysts not only facilitated diffusion of the reactants and products but could also lessen the amount of carbon deposited during reactions. As revealed by CO chemisorption, transmission electron microscopy (TEM), and X-ray photoelectron spectroscopy (XPS), the metal particles appeared to be partially covered by the alumina matrix (Al–O) due to the simultaneous formation of particles during FSP synthesis. Such phenomena, however, were shown to result in the formation of active Pt–Sn ensembles for propane dehydrogenation as shown by higher turnover frequencies (TOFs).



## 1. Introduction

Due to the uncertain oil price and the growing demand of propylene in the past few years, the catalytic dehydrogenation of propane from natural gas has received much attention as an alternative way for producing propylene. The dehydrogenation of propane is an endothermic reaction that requires high temperature, which promotes the thermal cracking reaction to coke and light alkane. The catalysts with high activity, high selectivity, and good stability are required to overcome this problem. Chromium- and platinum-based catalysts are most widely studied in such reactions [1]. However, both of them have relatively poor reaction stability due to the carbon deposits.

It is well known that addition of Sn to Pt-based catalysts can promote desired dehydrogenation reactions while inhibiting coking reactions [2–7]. The role of Sn in Pt–Sn catalyst has been explained in terms of geometric effects and/or electronic effects. For geometric effects, tin decreases the size of platinum ensembles, which reducing hydrogenolysis and coking reactions, while for electronic effects, tin modifies the electronic density of Pt, due either to a positive charge transfer from $Sn^{n+}$ species or to the different electronic structures of Pt–Sn alloys. This modification was responsible for changes in the heat of adsorption of different adsorbates participating in the reaction.

Bimetallic Pt and Sn supported on different supports, such as metal oxides ($Al_2O_3$, $ZrO_2$, $SiO_2$, $TiO_2$) [2,3,8–10], zeolites (ZSM-5) [11,12], and mesoporous materials (SBA-15) [13], which are believed to be the promising catalysts for propane dehydrogenation and thus have been extensively investigated. Among those, Pt–Sn/$Al_2O_3$ is one of the favorite dehydrogenation catalysts, owing to the strong interactions between Pt metal and $Al_2O_3$ supports, which could affect the reduction behavior and stability of the catalyst.

Flame synthesis, especially flame spray pyrolysis (FSP), is a relatively new process for one-step synthesis of supported metal catalysts. It is generally known as a method for making nanoparticles such as fume silica, titania, and carbon black in large quantities at low cost [14]. Many applications of supported metal catalysts synthesized via FSP method have been reported. For examples, flame-made Pt–Ba/$Al_2O_3$ and Pt/Ba/$Ce_xZr_{1-x}O_2$ have

* Corresponding author. Tel.: +66 8303 65411; fax: +66 3421 9368.
*E-mail address:* okornm@yahoo.com (O. Mekasuwandumrong).

0926-860X/$ – see front matter © 2009 Published by Elsevier B.V.
doi:10.1016/j.apcata.2009.08.006

been investigated in lean-$NO_x$ storage-reduction [15,16]. High surface area FSP-derived Ag/ZnO has been reported to exhibit high photocatalytic performance in UV-photodegradation of methylene blue [17]. Baiker et al. [18–20] successfully applied the FSP method for syntheses of various $Al_2O_3$-supported noble metal catalysts. The flame-made $Pt/Al_2O_3$ showed an improved turnover frequency in the hydrogenation of ethyl pyruvate compared to conventional porous catalysts. Our recent studies also show that $Pd/SiO_2$ synthesized in one-step by FSP method exhibited higher hydrogenation activity in the liquid-phase selective hydrogenation of 1-heptyne comparing to the ones prepared by a conventional impregnation method [21,22]. The structural differences of the flame-made and conventionally prepared catalysts have often been explained as the reasons for the differences in their catalytic behaviors.

One aim of this study is to extend our investigation to the flame-synthesized $Pt–Sn/Al_2O_3$ catalysts with 0.3 wt% Pt and 0.5–1.5 wt% Sn in the dehydrogenation of propane to propylene. The stronger metal–support interaction in the flame-made catalysts is believed to produce great beneficial effects in such reactions. The catalyst behaviors have been correlated with the characterization results obtained using $N_2$ physisorption, X-ray diffraction (XRD), CO pulse chemisorption, transmission electron spectroscopy (TEM), and X-ray photoelectron spectroscopy (XPS) techniques. The $Pt–Sn/Al_2O_3$ catalysts prepared by conventional impregnation of Pt and Sn precursors on both the flame-synthesized and the reference $Al_2O_3$ were also employed for comparison purposes.

## 2. Experimental

### 2.1. Catalyst preparation

#### 2.1.1. Flame-made catalysts

Synthesis of $Pt–Sn/Al_2O_3$ was carried out using a spray flame reactor similar to that of Ref. [23]. Platinum actetylacetonate, tin ethylhexanoate and aluminum butoxide from Aldrich were used as platinum, tin and aluminum precursors, respectively. Precursors were prepared by dissolving in xylene (MERCK; 99.8 vol.%) with total metal concentration maintained at 0.3 M. The platinum concentration was fixed at 0.3 wt% while the tin content was varied between 0.5 and 1.5 wt%. Using a syringe pump, 5 ml/min of precursor solution was dispersed into fine droplets by a gas-assisted nozzle fed by 5 l/min of oxygen (Thai Industrial Gas Limited; purity >99%). The pressure drop at the capillary tip was maintained at 1.5 bar by adjusting the orifice gap area at the nozzle. The spray was ignited by supporting flamelets fed with oxygen (3 l/min) and methane (1.5 l/min) which are positioned in a ring around the nozzle outlet. A sintered metal plate ring (8 mm wide, starting at a radius of 8 mm) provided an additional 10 l/min of oxygen as sheath for the supporting flame. The product particles were collected on a glass fiber filter (Whatman GF/C, 15 cm in diameter) with the aid of a vacuum pump.

#### 2.1.2. Impregnation-made catalysts

For comparison purposes, the impregnation-made $Pt–Sn/Al_2O_3$ catalysts were prepared by co-impregnation of the solution of platinum actetylacetonate and tin ethylhexanoate in xylene on a commercially available (Fluka) alumina and on the flame-made alumina. The metal content in these catalysts was 0.3% Pt and 1% Sn.

### 2.2. Catalyst characterization

X-ray diffraction (XRD) patterns were recorded with a Siemens D5000 using nickel filtered Cu Kα radiation. The crystallite size ($d_{XRD}$) was determined using the Scherrer equation and α-alumina as the external standard. The BET (Brunauer Emmett Teller) surface area, average pore size diameters, and pore size distribution were determined by physisorption of nitrogen ($N_2$) using a BEL-SORP automated system. The morphology and particle size of powders were observed using a JEOL-JEM 200CX transmission electron microscope operated at 100 kV. The active sites and relative percentage dispersions of platinum catalyst were determined by CO-pulse chemisorption technique using a Micromeritics Chemi-Sorb 2750 system running ChemiSoft TPx software at room temperature. XPS analysis was performed using an AMICUS photoelectron spectrometer equipped with a Mg Kα X-ray as a primary excitation and running KRATOS VISION2 software. XPS elemental spectra were acquired with 0.1 eV energy steps at a pass energy of 75 kV. The C1s line was taken as an internal standard at 285.0 eV.

### 2.3. Catalytic evaluation

The dehydrogenation of propane (Thai Industrial Gas) was carried out in a fixed-bed reactor with an inner diameter of 6 mm. Approximately 0.1 g of catalyst was loaded in the middle of the reactor. Prior to the experiments the catalysts were pretreated in flowing $H_2$ (30 ml/min) at 773 K for 1 h. The reaction was carried out isothermally at 823 K and at atmospheric pressure. The reaction mixture composed of $H_2$, $C_3H_8$ and Ar ($H_2/C_3H_8$/Ar molar ratio = 1:1:5) was fed to the reactor with the weight hourly space velocity (WHSV) based on propane of 5 $h^{-1}$. A purge gas (Ar) flow of 30 ml/min was used and the reaction mixture was preheated at 773 K. The product gases were analyzed on-line using a gas chromatograph with a TCD detector using a SUS Column PorapakQ, 80/100 mesh column.

## 3. Results and discussion

### 3.1. Catalyst properties

Fig. 1 shows the XRD patterns of impregnation- and flame-made $Pt/Al_2O_3$ and $Pt–Sn/Al_2O_3$ catalysts with Sn loadings 0.5–1.5 wt%. All the catalyst samples exhibited only the characteristic peaks of γ-$Al_2O_3$, additional peaks corresponding to Pt, Sn, and other alumina phases were not observed, probably due to the low amounts of Pt and Sn present and/or to the high dispersion of these metals on the $Al_2O_3$ supports. Addition of Pt or Sn simultaneously with Al during flame synthesis did not affect alumina phase transformation. Formation of γ-phase in high temperature flame can be explained by the fact that the particles spent only a few

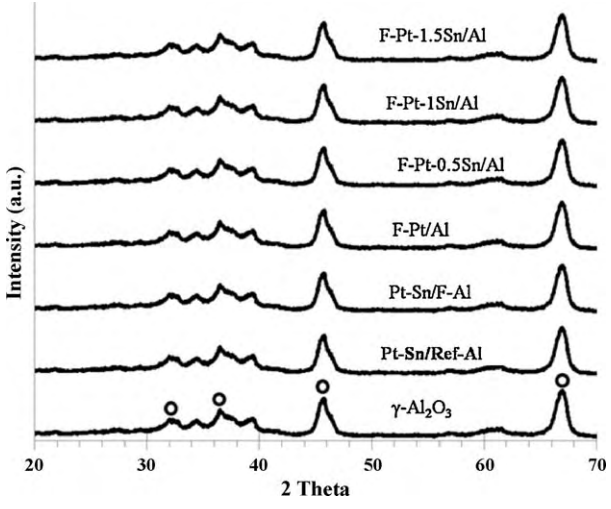


**Fig. 1.** XRD patterns of the flame-made $Pt–Sn/Al_2O_3$ catalysts (as synthesized).

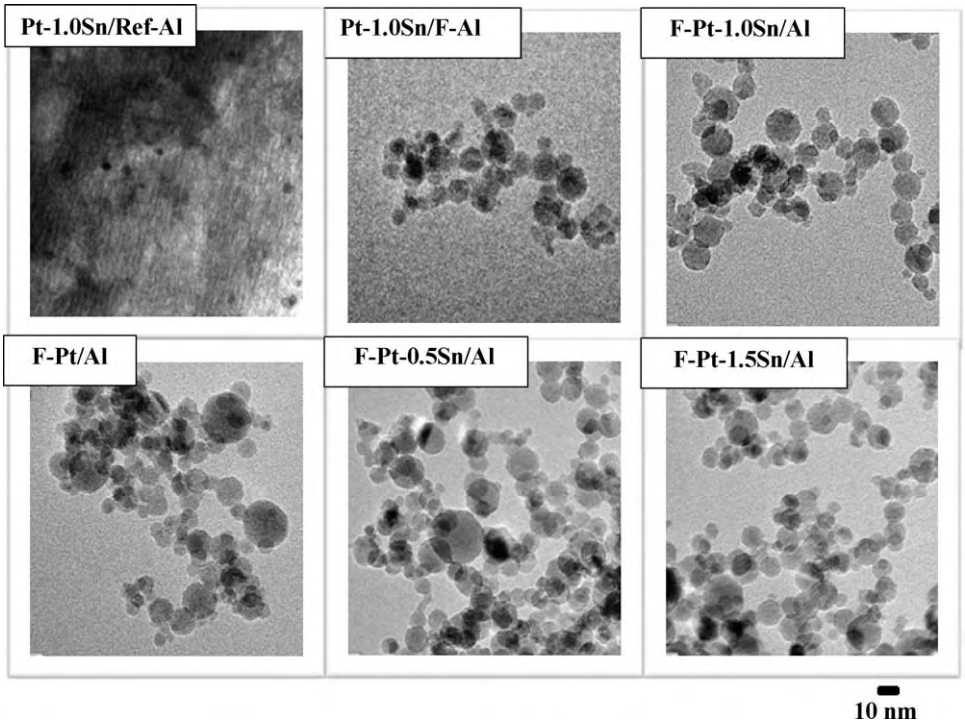


**Fig. 2.** TEM micrographs of the various flame- and impregnation-made Pt–Sn/$Al_2O_3$ catalysts.

seconds in the flame. This result is consistent with the work from Baiker et al. [18–20].

Typical TEM micrographs of the impregnated and flame-made Pt/$Al_2O_3$ and Pt–Sn/$Al_2O_3$ catalysts are shown in Fig. 2. The impregnation-made Pt–Sn supported on reference $Al_2O_3$ catalysts (Pt–1.0Sn/Com-Al) consisted of agglomerated large particles of alumina and spherical Pt/PtO particles/granules with average sizes between 2 and 5 nm dispersed on the alumina surface (shown as dark spots). The flame-made powder consisted of spherical primary particles with average sizes around 10–18 nm. Pt/PtO metal clusters were not distinguishable for the impregnation-made Pt–Sn on flame-made $Al_2O_3$ supports (Pt–1.0Sn/F–Al) and for all the flame-made catalysts.

Fig. 3 shows the XRD particle size ($d_{XRD}$) for $Al_2O_3$ (triangles), the BET equivalent particle size ($d_{BET}$; circles), and the average particle size obtained from TEM analysis ($d_{TEM}$; square) as a function of Sn loading for the flame-made Pt–Sn/$Al_2O_3$ powders.

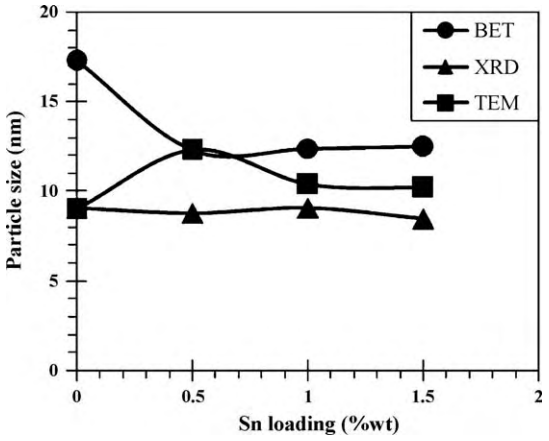


**Fig. 3.** XRD particle size ($d_{XRD}$) for $Al_2O_3$ (triangles), together with the BET equivalent particle size ($d_{BET}$; circles) and TEM particle size ($d_{TEM}$; square), as a function of Sn loading for Pt–Sn/$Al_2O_3$ powders.

The calculated $d_{BET}$ data were found to be in good agreement with the $d_{XRD}$ and $d_{TEM}$ values indicating that the particles were single crystalline. The physicochemical properties of the impregnation- and flame-made Pt–Sn/$Al_2O_3$ catalysts are summarized in Table 1. The BET surface areas of the reference and the flame-made $Al_2O_3$ supports were 145 and 105 $m^2/g$, respectively, whereas those of the corresponding impregnation-made Pt–Sn/$Al_2O_3$ catalysts were 139 and 103 $m^2/g$. A small decrease in BET surface area of the alumina supports can be explained by pore blockages during impregnation of platinum and tin precursors. On the other hand, the BET surface areas of flame-made Pt and Pt–Sn catalysts were ranged between 110 and 122 $m^2/g$, which were higher than the area of the flame-made $Al_2O_3$ support alone. Such a result suggests an inhibition of the growth of $Al_2O_3$ particles by Pt and Sn dopants resulting in formation of smaller particles. The $N_2$ adsorption–desorption isotherms (Fig. 4) reveal that the catalysts prepared in one-step by FSP and the impregnation-made catalysts supported on FSP-derived alumina contained only large pores and did not possess any mesopores, while the impregnation-made ones supported on reference alumina showed the properties of typical mesoporous materials.

The relative amounts of active Pt metals on the catalyst surface were calculated from CO chemisorption experiments at room temperature. The calculation of Pt active sites was based on the assumption that one carbon monoxide molecule adsorbs on one platinum site. Our preliminary tests of CO-pulse chemisorption indicated that flame-made Sn/$Al_2O_3$ and the $Al_2O_3$ support do not chemisorb CO. For the FSP-synthesized catalysts, the density of Pt active sites decreased from $2.3 \times 10^{18}$ to $1 \times 10^{18}$ sites/g-catalyst as Sn content increased from 0 to 1.5 wt%, corresponding to decreasing of Pt metal dispersion from 28 to 12.2%. As suggested by others, the lower amount of CO chemisorption on the Pt–Sn catalysts can be attributed to the formation of Pt–Sn ensembles or alloys that do not adsorb CO [24]. The average $Pt^0$ metal particle sizes calculated from CO chemisorption were in the range of 4–9 nm. Comparing the catalysts with similar metal composition (0.3 wt% Pt and 1.0 wt% Sn), we found the amount of Pt active sites

**Table 1**
Physicochemical properties of flame- and impregnation-made $Al_2O_3$ and Pt–Sn/$Al_2O_3$ catalysts.

| Catalyst | BET surface areas ($m^2$/g) | Total pore volume (cc/g) | Average pore diameter (nm) | CO chemisorption results | | | XPS B.E. (eV) Sn $3d_{5/2}$ | Atomic ratio Sn/Al |
|---|---|---|---|---|---|---|---|---|
| | | | | CO uptake (molecule CO/g cat.) | %Pt dispersion | $d_P$ $Pt^0$ (nm) | | |
| $Al_2O_3$ (Ref) | 145 | 0.29 | 13.1 | n/a | n/a | n/a | n/a | n/a |
| $Al_2O_3$ (FSP) | 104 | 0.42 | 64.2 | n/a | n/a | n/a | n/a | n/a |
| Pt–1.0Sn/Com-Al | 139 | 0.26 | 9.2 | $1.44 \times 10^{18}$ | 17.3 | 6.2 | 488.3 | 0.131 |
| Pt–1.0Sn/F–Al | 103 | 0.29 | 50.9 | $1.95 \times 10^{18}$ | 23.4 | 4.6 | 488.4 | 0.013 |
| F–Pt/Al | 110 | 0.37 | 63.7 | $2.32 \times 10^{18}$ | 28.0 | 3.9 | n/a | n/a |
| F–Pt–0.5Sn/Al | 122 | 0.36 | 63.5 | $1.75 \times 10^{18}$ | 21.0 | 5.1 | 486.1 | 0.002 |
| F–Pt–1Sn/Al | 112 | 0.31 | 59.2 | $1.22 \times 10^{18}$ | 14.6 | 7.4 | 486.7 | 0.005 |
| F–Pt–1.5Sn/Al | 120 | 0.31 | 56.0 | $1.01 \times 10^{18}$ | 12.2 | 8.8 | 486.5 | 0.010 |

to be dependent on the preparation method and on the different alumina supports used in the order: Pt–1.0Sn/F–Al > Pt–1.0Sn/Com-Al > F–Pt–1.0Sn/Al. It is also possible that the F–Pt–1.0Sn/Al catalyst, which was prepared by one-step FSP method exhibited CO chemisorption suppression due to the formation of an alumina matrix (i.e., in the form of Al–O groups) covering the Pt and Sn surfaces during FSP synthesis.

Surface compositions in term of Sn/Al atomic ratios of the various FSP- and impregnation-made Pt–Sn/$Al_2O_3$ catalysts were determined by XPS technique, the results are given in Table 1. It was found that the Sn/Al atomic ratio for Pt–Sn/Com-Al catalyst was ten and twenty-five times higher than those of Pt–Sn/F–Al and F–Pt–Sn/Al, respectively. For the impregnation-made catalysts, the larger pore size of FSP-made alumina made it possible for Pt and Sn particles to be located deeper inside the pores than was possible for the reference $Al_2O_3$-supported ones. For the FSP-made catalysts, it is likely that the metals were partially covered by the $Al_2O_3$ matrix during one-step FSP synthesis resulting in much lower Sn/Al ratio observed. It should, however, be noted that Pt species were not detected in all cases due to the very low amount present.

The XPS elemental scan peak for Sn $3d_{5/2}$ was observed at 488.3–488.4 eV for impregnation-made Pt–Sn/$Al_2O_3$ catalysts, while the FSP-made catalysts exhibited the characteristic peak corresponding to oxidized Sn species at 486.1–486.7 eV. According to the literature data, a binding energy at 486.5–486.9 eV represents $Sn^{2+}$, while $Sn^{4+}$ exhibits higher binding energies at 486.5–488.0 eV [25–27]. The lower binding energies of Sn $3d_{5/2}$ for the FSP-made catalysts thus suggest that the more reducible form of Sn was produced in the Pt–Sn/$Al_2O_3$ catalysts synthesized by the one-step FSP method.

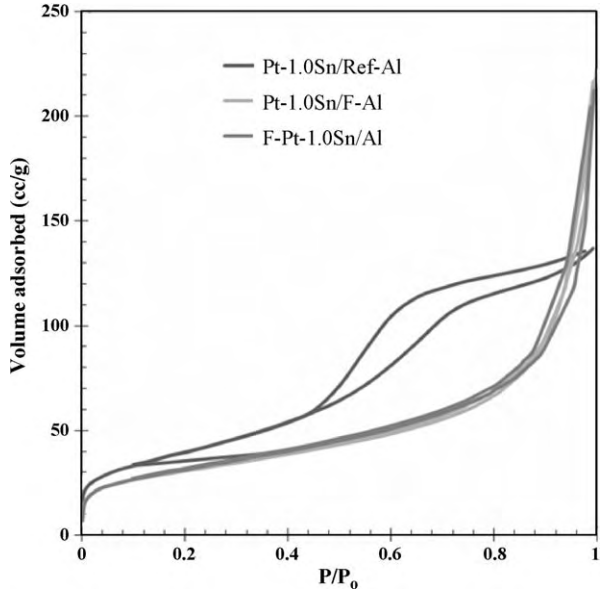


**Fig. 4.** $N_2$ physisorption isotherms of the flame- and impregnation-made catalysts.

Particle formation during FSP synthesis of supported noble metals has been suggested earlier [15,28]. According to the proposed mechanism, formation of FSP-made Pt–Sn/$Al_2O_3$ nanoparticles can be considered as follows: the sprayed droplets of precursor solution were evaporated and combusted as soon as they met the flame at very high temperature and released the metal atoms; then nucleation and growth of particles by coagulation and condensation occurred along the axial direction of the flame. Since the vapor pressure of $Al_2O_3$ was lower than those of the metals, the formation of $Al_2O_3$ particles could start earlier. Further downstream of the flame at lower temperature, Pt and Sn started to form small particles and/or deposits directly on the $Al_2O_3$ support. However, in such a very high temperature environment, it is likely that some of the metal particles were covered by support matrix.

### 3.2. Catalyst behavior in the dehydrogenation of propane

The catalytic behaviors of the flame-made Pt/$Al_2O_3$ and Pt–Sn/$Al_2O_3$catalysts were investigated in the dehydrogenation of propane reaction. The catalytic performance in terms of propane conversion, selectivity to propene, and the turnover frequencies (TOFs) calculated based on CO chemisorption of the flame-made Pt/$Al_2O_3$ and Pt–Sn/$Al_2O_3$catalysts are given in Table 2. The results were compared to those of the impregnation-made Pt–Sn supported on flame-made and reference $Al_2O_3$ supports. The conversion of propane for the flame-made Pt/$Al_2O_3$ and Pt–Sn/$Al_2O_3$catalysts increased from 7.3 to 22.6% as Sn loading increased from 0 to 0.5 wt% and decreased to 12.7% when Sn loading was increased further to 1.5 wt%. When there was an excessive amount of Sn on the catalyst surface, a larger amount of $Sn^0$ species could be produced, resulting in an alloy formation, and as a consequence the catalyst activity decreased [11,12]. However, this was probably not the case in this study, since there was no significant change in the binding energies of Sn species for the FSP-derived Pt–Sn/$Al_2O_3$ catalysts with various Sn contents. On the other hand, the Sn/Al atomic ratio for F–Pt–1.5Sn/Al was found to be much higher than

**Table 2**
Catalytic properties for propane dehydrogenation.

| Catalyst | % Conversion | | %$C_3H_6$ selectivity | TOFs ($s^{-1}$)[a] |
|---|---|---|---|---|
| | Initial | Final | | |
| Pt–1.0Sn/Ref-Al | 6.6 | 5.1 | 97 | 0.9 |
| Pt–1.0Sn/F–Al | 25.3 | 15.1 | 97 | 2.6 |
| F–Pt/Al | 11.8 | 7.3 | 98 | 1.1 |
| F–Pt–0.5Sn/Al | 33.8 | 22.6 | 99 | 3.7 |
| F–Pt–1.0Sn/Al | 29.1 | 17.8 | 97 | 4.7 |
| F–Pt–1.5Sn/Al | 18.8 | 12.6 | 98 | 3.5 |

[a] TOF = mole product/mole Pt metal/s (based on CO chemisorption results).

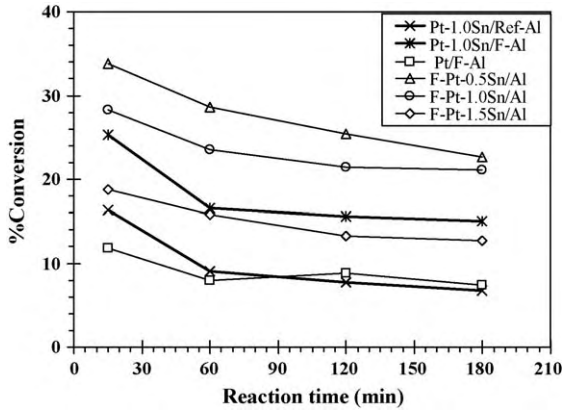


**Fig. 5.** Plot between propane conversion and reaction time of all the catalysts.

the others, suggesting the possibility for blockages of active Pt surface by excessive amount of Sn and/or the decrease in acidity of the alumina support, which would also lower the catalyst activity [11,12]. Comparing the catalysts prepared by different techniques (similar Sn content), we find that the propane conversion was improved in the order: F–Pt–1.0Sn/Al > Pt–1.0Sn/F–Al > Pt–1.0Sn/Com-Al. There was no significant difference in the selectivity for propylene for all the $Pt/Al_2O_3$ and $Pt–Sn/Al_2O_3$catalysts (propylene selectivity ≈96–99%). It should be noted that the calculated TOF for F–Pt–1.0Sn/Al catalyst was approximately two-fold and five-fold higher than those of the impregnation-made ones supported on flame-made and reference alumina, respectively. In other words, the simultaneous formation of $Pt–Sn/Al_2O_3$ nanoparticles by FSP method could produce highly active Pt–Sn ensembles for such reaction.

The relations between propane conversion and reaction time are plotted in Fig. 5. The propane conversion was gradually decreased during 180 min time-on-stream in all cases, suggesting catalyst deactivation due probably to coke formation. The percentages of catalyst activity change are shown in Fig. 6. Compared to the conventional impregnation-made ones, all the flame-made catalysts exhibited better stability with the F–Pt–1.0Sn/Al showing the lowest deactivation. The lower catalyst deactivation rate for the FSP-made catalysts can be attributed to their larger pore size, resulting in lower amounts of coke formation and/or less carbon blocking active sites. Considering the FSP-catalysts with different Sn contents, we found that the percent deactivation decreased from 37.5 to 25% as Sn loading

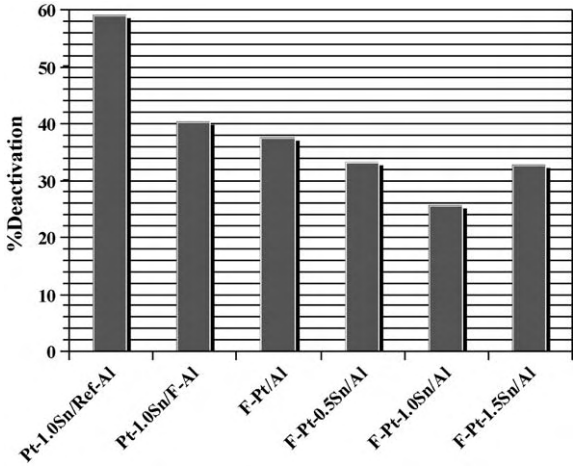


**Fig. 6.** Percentages of the catalyst activity change for flame- and impregnation-made catalysts.

increased from 0 to 1 wt% and then decreased to 32.5% when the amount of Sn was further increased to 1.5%. It is known that there are two active centers (metal and acid sites) for the $Pt/Al_2O_3$ catalysts. Pt is used as the hydrogenation center, while the acid sites on $Al_2O_3$ support are "double-faced". When the balance of metal and acid of the catalysts is kept, the synergistic effect is beneficial to the dehydrogenation activity and catalyst stability. When the acidity is strong, the acid sites promote the undesired reactions such as cracking, isomerization and polymerization, which decreased the olefin selectivity and stability of the catalyst [29,30]. There exists an optimum ratio between the number of acid sites and the number of active metal sites on the catalyst surface in order to improve activity and stability of the catalysts. Addition of an appropriate amount of Sn would adjust the ratio between these two sites so that better catalyst performance was obtained.

## 4. Conclusions

The $Pt–Sn/Al_2O_3$ catalysts synthesized by one-step FSP method exhibited higher catalytic activity and better stability in the dehydrogenation of propane with high propylene selectivity (≥96%) compared to the ones prepared by conventional impregnation of Pt and Sn precursors on either the flame-made or the reference $Al_2O_3$ supports. Addition of Pt and Sn simultaneously with Al during FSP synthesis produced single crystalline γ-alumina particles with the as-prepared primary particle size of 10–18 nm. An optimum Sn loading that yielded the highest catalyst activity and lowest catalyst deactivation rate was determined to be ca. 1 wt%. The better catalytic performance and stability of the FSP-derived $Pt–Sn/Al_2O_3$ catalysts were attributed to the formation of highly active Pt–Sn ensembles and to the very large pore sizes of the flame-made catalysts, respectively.

## Acknowledgements

The authors would like to express their thanks for the financial supports from Development Institute of Silpakorn University, Commission on Higher Education, the Thailand Research Fund (TRF) and Cooperation on Science and Technology Researchers Development Project by Office of the Permanent Secretary Ministry of Science and Technology.

## References

[1] M.M. Bhasin, J.H. McCain, B.V. Vora, T. Imai, P.R. Pujado, Appl. Catal. A: Gen. 221 (2001) 397.
[2] P. Praserthdam, N. Grisdanurak, W. Yuangsawatdikul, Chem. Eng. J. 77 (2000) 215.
[3] O.A. Bariás, A. Holmen, E.A. Blekkan, J. Catal. 158 (1996) 1.
[4] S.B. Kogan, H. Schramm, M. Herskowitz, Appl. Catal. A: Gen. 208 (2001) 185.
[5] J. Salmones, J. Wang, J.A. Galicia, G. Aguilar-Rios, J. Mol. Catal. A: Chem. 184 (2002) 203.
[6] L. Bednarova, C.E. Lyman, E. Rytter, A. Holmen, J. Catal. 211 (2002) 335.
[7] M. Larsson, M. Hultén, E.A. Blekkan, B. Andersson, J. Catal. 164 (1996) 44.
[8] S.B. Kogan, H. Schramm, M. Herskowitz, Stud. Surf. Sci. Catal. 88 (1994) 519–524.
[9] C. Larese, J.M. Campos-Martin, J.J. Calvino, G. Blanco, J.L.G. Fierro, Z.C. Kang, J. Catal. 208 (2002) 467–478.
[10] A. Vázquez-Zaval, A. Ostoa-Montes, D. Acosta, A. Gómez-Cortés, App. Surf. Sci. 136 (1998) 62–72.
[11] Y. Zhang, Y. Zhou, A. Qiu, Y. Wang, Y. Xu, P. Wu, Catal. Commun. 7 (2006) 860–866.
[12] Y. Zhang, Y. Zhou, K. Yang, Y. Li, Y. Wang, Y. Xu, P. Wu, Micropor. Mesopor. Mater. 96 (2006) 245.
[13] L. Huang, B. Xu, L. Yang, Y. Fan, Catal. Commun. 9 (2008) 2593.
[14] W.J. Stark, S.E. Pratsinis, Powder Technol. 126 (2002) 103.
[15] M. Piacentini, R. Strobel, M. Maciejewski, S.E. Pratsinis, A. Baiker, J. Catal. 243 (2006) 43.
[16] R. Strobel, F. Krumeich, S.E. Pratsinis, A. Baiker, J. Catal. 243 (2006) 229.
[17] M.J. Height, S.E. Pratsinis, O. Mekasuwandunrong, P. Praserthdam, Appl. Catal. B: Environ. 63 (2006) 305.
[18] R. Strobel, W.J. Stark, L. Madler, S.E. Pratsinis, A. Baiker, J. Catal. 213 (2003) 296.
[19] R. Strobel, F. Krumeich, W.J. Stark, S.E. Pratsinis, A. Baiker, J. Catal. 222 (2004) 307.
[20] S. Hannemann, J.-D. Grunwaldt, P. Lienemann, D. Gunther, F. Krumeich, S.E. Pratsinis, A. Baiker, Appl. Catal. A: Gen. 316 (2007) 226.

[21] S. Somboonthanakij, O. Mekasuwandumrong, J. Panpranot, T. Nimmanwudtipong, R. Strobel, S.E. Pratsinis, P. Praserthdam, Catal. Lett. 119 (2007) 346.
[22] O. Mekasuwandumrong, S. Somboonthanakij, P. Praserthdam, J. Panpranot, Ind. Eng. Chem. Res. 48 (2009) 2819.
[23] R. Strobel, A. Baiker, S.E. Pratsinis, Adv. Powder Technol. 17 (2006) 457.
[24] S.M. Stagg, C.A. Querini, W.E. Alvarez, D.E. Resasco, J. Catal. 168 (1997) 75.
[25] J. Homs, M. Llorca, J. Jolis Riera, J. Fierro, J. Sales, P. Ramírez de la Piscina, J. Mol. Catal. A: Chem. 200 (2003) 251.
[26] A. Huidobro, A. Sepúlveda-Escribano, F. Rodríguez-Reinoso, J. Catal. 212 (2002) 94.
[27] E. Merlen, P. Beccat, J.C. Bertolini, P. Delichere, N. Zanier, B. Didillon, J. Catal. 159 (1996) 178.
[28] W.Y. Teoh, L. Mädler, D. Beydoun, S.E. Pratsinis, R. Amal, Chem. Eng. Sci. 60 (2005) 5852.
[29] L.W. Lin, T. Zhang, J.L. Zang, Z.S. Xu, Appl. Catal. A: Gen. 67 (1990) 11.
[30] S. He, C. Suna, Z. Bai, X. Dai, B. Wang, Appl. Catal. A: Gen. 356 (2009) 88.